SPECIAL SECTION: ORIGINAL ARTICLE

Strong near-inertial oscillations in geostrophic shear in the northern South China Sea

Zhenyu Sun · Jianyu Hu · Quanan Zheng ·
Chunyan Li

Abstract With observational data from three Acoustic
Doppler Current Profiler (ADCP) moorings, we detected
strong near-inertial oscillations (NIO) in the continental
shelf region of the northern South China Sea in July 2008.
The amplitude of the near-inertial current velocity is much
greater than that of diurnal and semi-diurnal tides. The
power of the NIOs is strongest in the intermediate layer,
relatively weak in the surface layer, and insignificant in the
near-bottom layer. The spectral analysis indicates that the
NIOs have a peak frequency of 0.0307 cph, which is 2%
lower than the local inertial frequency, i.e., a red-shift. The
near-inertial wave has an upward vertical phase velocity,
which involves a downward group velocity and energy
flux. The estimated vertical phase velocity is about
43 m day^{-1}, corresponding to a vertical wave length of
about 58 m. The horizontal scale of the NIOs is at least
hundreds of kilometers. This NIO event lasted for about
15 days after a typhoon's passage. Given the northeastward
background flow with significant horizontal shear, both
Doppler shift and shear flow modulation mechanisms may
be responsible for the red-shift of the observed NIOs. For
the shear flow mechanism, the observed negative back-
ground vorticity and the corresponding effective Coriolis

frequency reduce the lower limit of admissible frequency
band for the NIOs, causing the red-shift. Meanwhile, the
mooring area with the broadened frequency band acts as a
wave-guide. The trapping and amplification effects lead to
the relatively long sustaining period of the observed NIOs.

1 Introduction

Oceanic near-inertial oscillation (NIO) is the intrinsic
motion when the inertia of sea water is mainly balanced by
the Coriolis force. Observations of oceanic current have
demonstrated its frequent occurrences in the global ocean
(Webster 1968). Its typical manifestation is the intensified
oscillating rotary current with a peak frequency near the
local Coriolis frequency f, where $f = 2\Omega\sin\theta$, Ω is the
angular speed of the earth's rotation, and θ is the local
latitude. Theoretical models of NIO were established and
have shown results consistent with observations (Pollard
1970; Gill 1984).

The NIOs have the following characteristics (Fu 1981):
(1) they have a horizontal coherent scale of at least several
kilometers and a vertical coherent scale of only tens of
meters. (2) The oscillation frequency is not exactly the
local inertial frequency f. Most of the occasions have a
frequency slightly above f, which is referred to as blue-
shift, while fewer occasions have a frequency slightly
below f, i.e., red-shift. (3) In the vertical direction, an
upward phase velocity and a downward group velocity are
dominant. The characteristics of NIOs in a mean flow with
or without geostrophic shears have been analyzed under the
theory of linear waves (Orvik and Mork 1995; Mooers

Z. Sun (✉) · J. Hu
State Key Laboratory of Marine Environmental Science,
Xiamen University, Xiamen 361005, Fujian, China
e-mail: sunzy@xmu.edu.cn

Q. Zheng
Department of Atmospheric and Oceanic Science,
University of Maryland, College Park, MD 20742, USA

C. Li
Department of Oceanography and Coastal Science,
Coastal Studies Institute, Louisiana State University,
Baton Rouge, LA 70803, USA

1975; Kunze 1985). Doppler shift is supposed to happen because of the wave-current interaction, and the background vorticity can also modify the frequency band of the NIOs.

Based on the current velocity data at mixed layer by Argo floats and surface drifters, Park et al. (2005) and Chaigneau et al. (2008) estimated the NIO distribution in the global ocean. The globally average surface velocity of the near-inertial component is about 10 cm s^{-1}, and the average velocity in mid-latitude areas is greater than that in the tropical and polar areas. NIOs can be triggered by atmospheric forcing and other oceanic processes, especially by strong disturbance from hurricanes (or typhoons). Numerous field observations revealed strong near-inertial current in the wake of hurricanes (Shay and Elsberry 1987; Zheng et al. 2006; Xie et al. 2009). The induced NIOs take place immediately after the hurricane's passage, and last for several or more than 10 days.

The South China Sea (SCS), which is located in the west of the tropical Pacific, has frequent typhoon and tropical storm events, averaging up to 15 occurrences per year according to historical records (e.g., typhoon records by Unisys Corp.). In addition, the SCS has variable hydrographic structures and circulation patterns because of the alternating monsoon. The effects of topography, stratification, and background flow are supposed to have significant influence on the characteristics of the NIOs. Many case studies of NIOs in the SCS have been presented (Chu et al. 2000; Zhang et al. 2005; Zhu and Li 2007), while studies on influences of hydrographic structure and background flow on the NIOs are relatively scarce.

In this study, we use the current velocity data from moored Acoustic Doppler Current Profilers (ADCPs) to present the strong NIOs on the continental shelf of northern SCS in 2008. The influence of the local background flow on the NIOs is analyzed, and finally we examine the relation between the NIOs and the preceding Typhoon "Fengshen."

2 Data

During the SCS Coastal Oceanographic Process Experiment (SCOPE) in July 2008, we deployed ADCP moorings at three stations (S205, S206 and S305) in the continental shelf region of the northern SCS (Fig. 1). The depths of these three stations range from 67 to 85 m. The three stations comprise a triangle. The line of S205 and S206 is normal to the isobath, while the line of S206 and S305 is along the isobath. Such an arrangement was intended to measure the cross-shore and alongshore current variation. Each mooring was equipped with a Teledyne RDI 300K ADCP to continuously record the current profiles from the bottom to the surface. Table 1 lists the details of three moorings, including their time ranges and instrument settings. After data quality control, we acquire the time series of the current profiles at each station for about 10 days starting from 1 July 2008. The current velocities are then decomposed into east and north components for further analysis.

As the Typhoon "Fengshen" passed by our study area several days before the mooring observation, we use the typhoon data to demonstrate the relation between the observed NIOs and the atmospheric forcing. The information about the typhoon, such as trajectory and wind speed, was obtained from Unisys (http://weather.unisys.com/hurricane).

Fig. 1 ADCP mooring stations (*red dots*) in the continental shelf region of northern SCS (isobath in meters) in July 2008. The schematic patterns of YCC and SCSWC (*black arrows*) and the trajectory (*grey line*) of Typhoon "Fengshen" in June 2008 are also denoted in the map
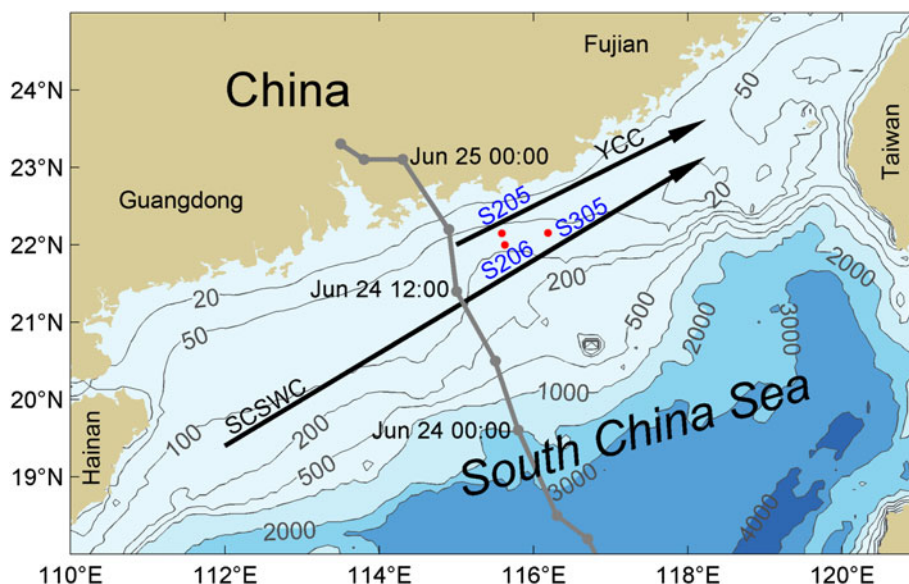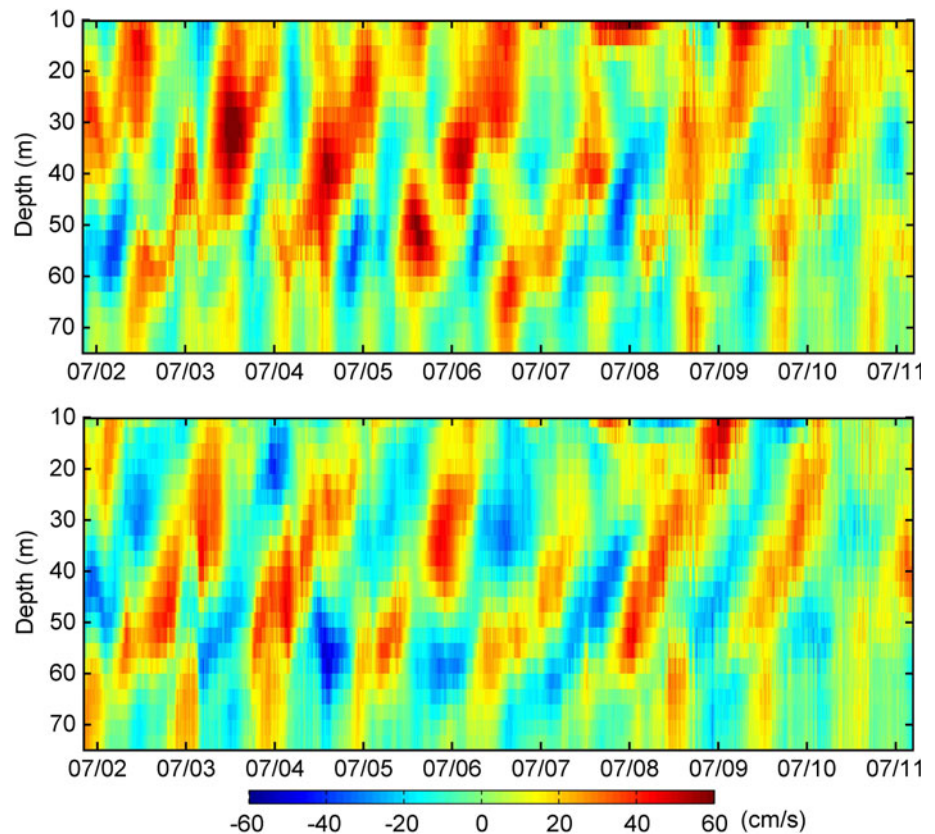
Table 1 Details of the ADCP moorings at the three stations in July 2008

Station	S205	S206	S305
Latitude	22.15°N	21.99°N	22.15°N
Longitude	115.59°E	115.62°E	116.18°E
Depth (m)	67	85	75
Instrument	RDI 300K ADCP	RDI 300K ADCP	RDI 300K ADCP
Time range	July 1–12	July 1–12	July 1–17
Depth range of available data (m)	6–56	9–75	6–40
Vertical sampling interval (m)	2	3	2
Temporal sampling interval (min)	1	10	20

Fig. 2 Time series of current profiles from 1 to 11 July at station S206 (*upper panel* for east current component and *lower panel* for north current component)

3 Near-inertial oscillations from the ADCP observations

Figure 2 shows the time series of current profiles at station S206. As indicated by the pattern of tilted stripes, the dominant current component at station S206 is a periodic oscillation, with a frequency apparently lower than that of diurnal tide. The local inertial frequency f is 0.0313 cph, corresponding to a period of 31.95 h. As the oscillation frequency is close to f, we determine it as an NIO. The magnitude of the oscillation is about 40 cm s^{-1} for both the east and north current components. The tilting direction of the stripes in Fig. 2 indicates an upward phase velocity in the vertical direction, i.e., the wave propagates from near-bottom to surface. The upward phase velocity involves a downward group velocity, implying downward energy propagation (Leaman and Sanford 1975; D'Asaro and Perkins 1984). The time series of currents at S205 and S305 have similar NIOs of the magnitudes and phase propagation (not shown).

We applied spectral analysis to the time series of observed current. The power spectra of the east and north current components at station S206 are calculated with a degree of freedom of 6 (Chen and Ma 1991). Figure 3 shows the power spectra at all levels from 10 to 75 m. There are three frequency bands in which the current power is concentrated, representing NIO (close to f in Fig. 4), diurnal (K_1) and semi-diurnal (M_2) tides. One can see that the power in near-inertial frequency band is greater than that in the diurnal and semi-diurnal bands. Along the vertical profile

Fig. 3 Power spectra [in (cm/ s)²/cph] of east and north current components at all levels at station S206 (*left panel* for east current component and *right panel* for north current component). Inertial frequency (*f*), diurnal frequency (K_1), and semidiurnal frequency (M_2) are denoted in the figure
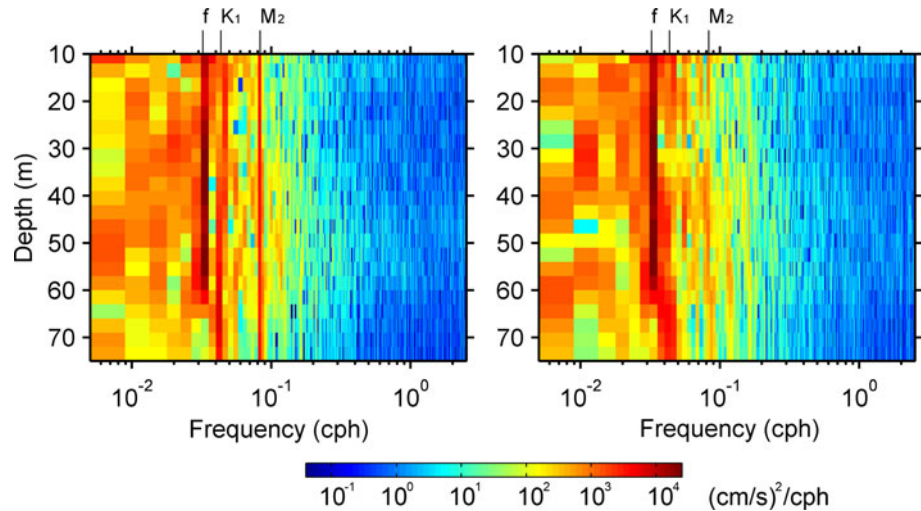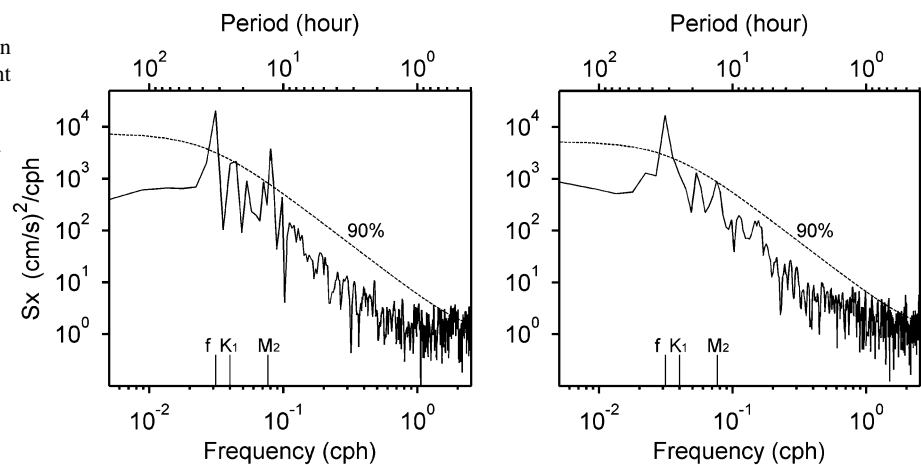
Fig. 4 Power spectra of east and north current components at 40-m depth at station S206 (*left panel* for east current component and *right panel* for north current component). Inertial frequency (*f*), diurnal frequency (K_1), and semidiurnal frequency (M_2) are denoted in the figure

(Fig. 3), the near-inertial band has the strongest power in the intermediate layer from 25 to 60 m, is relatively weak in the upper layer above 25 m, and is insignificant in the lower layer below 60 m. In comparison, the diurnal and semi-diurnal tides have much smaller magnitudes, and their power is more evenly distributed in the vertical profile. Taking 40 m as a typical depth of the intermediate layer, the spectrum at 40 m depth is shown in Fig. 4. One can see that the powers at near-inertial frequency of east and north current components are greater than 1×10^4 (cm s^{-1})^2 cph^{-1}, while the semi-diurnal tide only has a peak value of 4×10^3 (cm s^{-1})^2 cph^{-1} for the east current component. Therefore, the NIO is clearly the dominant current component, and this is also the case at stations S205 and S305.

To calculate the accurate peak frequency of the NIOs, we fit the time series of east and north current components to the following equation

$$U(t) = a_0 + a_1 \cos(2\pi f_P t) + b_1 \sin(2\pi f_P t) + E(t), \quad (1)$$

where $U(t)$ is the time series, a_0, a_1, b_1, and f_P are the parameters to be fitted, and $E(t)$ is the residual. The

resultant peak frequency f_P has no significant variation along the vertical profile and has an average value of 0.0307 cph for both the east and north current components, corresponding to a period of 32.58 h. This frequency is slightly lower than the local inertial frequency, i.e., $f_P = 0.98f$. The results derived from the other two stations (S205 and S305) are the same. In short, the observed NIOs have a peak frequency slightly below *f*, which represents a red-shift.

Linear internal wave dynamics, with constant *f* and no mean currents, admit wave solutions with frequencies higher than *f* and lower than *N* (e.g., Xu 1999), where *N* is the buoyancy frequency. In most cases, NIOs exhibit peak frequencies slightly higher than *f*, i.e., blue-shift (Gonella 1971; Perkins 1972), while occasions of red-shifts do exist (Perkins 1976; Fu 1981), which can be attributed to the wave-current interaction mechanisms for NIOs in background flows, such as Doppler shift and mean shear flow modulation. Orvik and Mork (1995) examined the Doppler shift of NIOs in the Norwegian Coastal Current by a two-layer model. In the uniform background flow, the

Doppler-shifted dispersion relation for the upstream propagating waves shows frequencies slightly below f in the long wave band. As for NIOs in the non-uniform background flows, internal wave dynamics indicate that background vorticity ζ, which is considerable in regions with geostrophic shear, shifts the lower bound of the internal wave band from f to an effective Coriolis frequency f_{eff}. Trapping and amplification of NIOs are supposed to occur in regions of negative vorticity according to the ray theory (Mooers 1975; Kunze 1985).

In the study area, the background flow consists of the Yuedong Coastal Current (YCC) and South China Sea Warm Current (SCSWC) during the summer monsoon season, as schematically shown in Fig. 1 (Hu et al. 2000, 2010; Su 2004). Therefore, both Doppler shift and mean shear modulation would adjust the wave properties of the observed NIOs. Figure 5 shows the mean flow profiles at the three stations during the mooring observation period. One can see that the northeastward mean flow is dominent at all three stations. The locations and flow magnitudes indicate that station S205 is close to the flow axis of YCC, and stations S206 and S305 are located on the south side of the current. The Doppler shift induced by the northeastward flow can be responsible for the decrease of the lower frequency limit of the upstream components of the NIOs, which can lead to the red-shift of the NIO frequency in our observations.

As for the effects of the mean shear, we use the three mean flow profiles measured by the moorings to estimate the background vorticity according to the following equation.

$$\zeta = \frac{\partial v}{\partial x} - \frac{\partial u}{\partial y}, \tag{2}$$

where x and y are alongshore and cross-shore coordinates, and u and v are alongshore and cross-shore current components, respectively. $\frac{\partial u}{\partial y}$ can be estimated by the current difference between stations S205 and S206, while $\frac{\partial v}{\partial x}$ by the difference between stations S206 and S305. We use the following equation (Perkins 1976) to calculate the effective Coriolis frequency f_{eff};
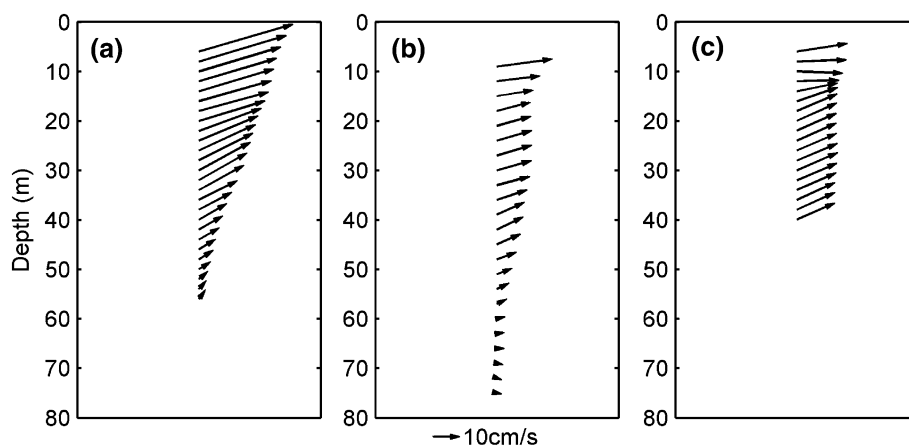
$$f_{\text{eff}}^2 = f(f + \zeta). \tag{3}$$

The resultant profiles of ζ and f_{eff} are shown in Fig. 6. The background flow has a negative vorticity profile, with the minimum vorticity of $-0.17f$ at the near-surface layer. Such a ζ profile leads to an f_{eff} profile smaller than f. Thus, the lower bound of the frequency band of NIOs in the study area is adjusted below f, which is likely to induce the frequency red-shift. The strong magnitude of the observed NIOs can also be attributed to the negative background ζ and adjusted f_{eff}, as the region with negative vorticity acts as a wave-guide and traps the incident NIOs from the nearby areas.

4 Estimation of phase velocity and spatial scales

Before estimating the phase velocity of the NIOs, we apply a band-pass filtering to the current time series by Fourier transform to extract the near-inertial components. The filtered current velocities at station S206 are shown in Fig. 7. The extracted NIOs have the patterns with clear periodic stripes in the current time series. The maximum amplitude of the oscillation occurs in the intermediate layer, but weak amplitude in the surface layer, while the oscillation in the near-bottom layer is insignificant. The horizontal current vector along the vertical profile rotates clockwise from the upper layer to lower layer, indicating an Ekman spiral.

To obtain an accurate estimate of the vertical phase velocity, we employ the Radon transform, which is widely used in the field of image processing to detect and extract lines in images (Deans 1983). The estimated vertical velocities based on the east and north current components are 42.6 and 43.5 m day^{-1}, respectively. With the oscillation period given in Sect. 3, the vertical wave length is

Fig. 5 Vertical profiles of the mean flow at the three mooring stations: **a** S205, **b** S206, and **c** S305

about 58 m. Horizontal scales are usually estimated by the phase difference and horizontal distance between stations. The phase profiles at the three stations are derived from the
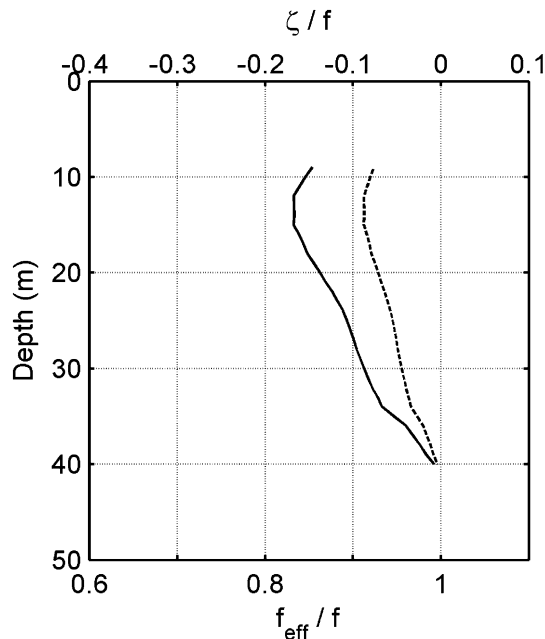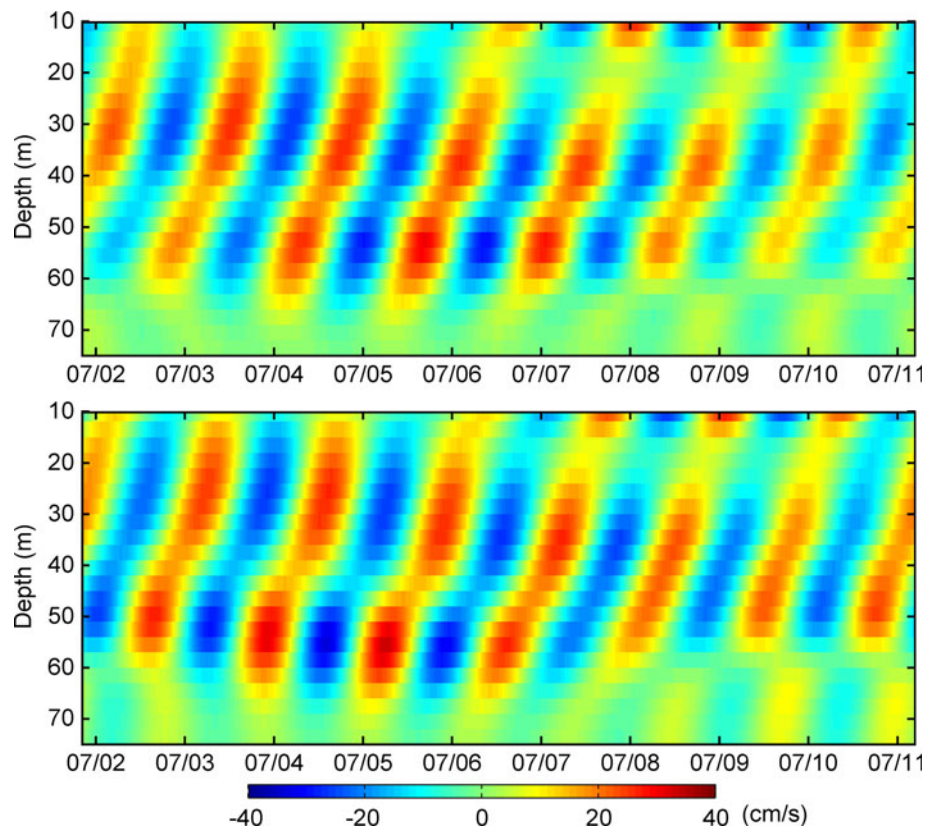

Fig. 6 Vertical profiles of the vorticity (*solid line*) and effective inertial frequency (*dashed line*) in the mooring area. Both profiles are normalized against the local inertial frequency f
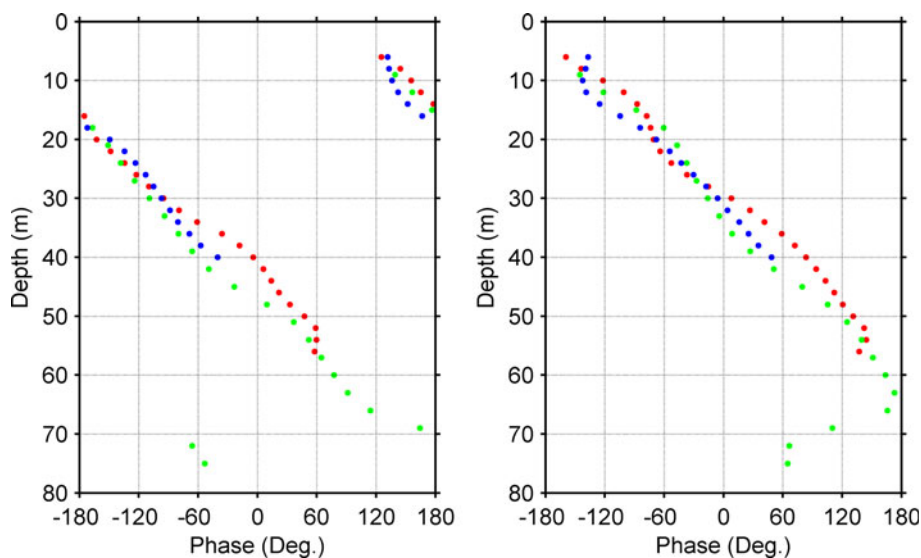
fitting results in Sect. 3 and are shown in Fig. 8. The three stations generally have phase profiles increasing with depth. Since a larger value of phase means a leading wave, one can see that the near-inertial currents at lower levels oscillate in advance of those at upper levels. At corresponding levels, phase differences among the three stations are insignificant. Therefore, the accurate horizontal spatial scale L can not be estimated by $L = 2\pi D/\Delta p$, where D is the horizontal distance between stations and Δp is the phase difference between stations. Given that D is tens of kilometers, the horizontal scale of the NIO is at least hundreds of kilometers.

5 Near-inertial oscillation and Typhoon "Fengshen"

Many factors can induce NIOs in the ocean, such as disturbance by atmospheric forcing and energy cascading from a meso-scale eddy (Fu 1981). Numerous case studies on oceanic response to hurricanes (or typhoons) indicated that hurricanes are an important cause of oceanic NIOs (e.g., Shay and Elsberry 1987; Zheng et al. 2006). Given the coincidence of our mooring observation and the preceding Typhoon "Fengshen" in June 2008, the observed strong NIOs were also triggered by the typhoon's disturbance. The category 2 Typhoon "Fengshen" originated in

Fig. 7 Band-pass filtered time series of the current profiles from 1 to 11 July at station S206 (*upper panel* for east current component and *lower panel* for north current component)

Fig. 8 Phase profiles of the near-inertial current component (*left panel* for east current component and *right panel* for north current component) of the three stations (*red* for station S205, *green* for station S206, and *blue* for station S305; larger phase means leading)

the west Pacific on 19 June 2008. It degraded to a tropical storm after entering the northern SCS and landed on the coast of Guangdong Province, China, on 25 June (trajectory shown in Fig. 1). Before its landing, "Fengshen" passed by our mooring area with a maximum wind speed of 25 m s^{-1}. The minimum distance from the mooring stations to the typhoon track is about 80 km. After the strong disturbance of "Fengshen," no significant atmospheric process occurred until the end of our mooring observation. As the moorings were deployed after the typhoon's passage, the data did not include the immediate oceanic response to "Fengshen." While our observation started from 6 days later, strong near-inertial currents still existed at that time. According to the time series in Fig. 7, the strong NIO did not begin to weaken until 9 July, indicating that this NIO event lasted for about 15 days after the typhoon's passage. This relatively long sustaining period can also be attributed to the trapping and amplification effects, as the negative background vorticity preserved the near-inertial energy from horizontal dispersion.

6 Summary and discussion

By the current velocity data from the ADCP moorings, we characterized the strong NIO in response to Typhoon "Fengshen" on the continental shelf of northern SCS in July 2008. Near-inertial currents at the mooring stations have oscillation amplitudes of about 40 cm s^{-1}, overwhelming the current components of diurnal and semidiurnal tides. Such strong occurrences in the SCS are scarcely reported by previous studies. The power of the NIOs is not evenly distributed along the vertical profile. It is evident that the intermediate layer has the largest amplitude of NIOs, whereas the near-bottom layer has no

significant oscillation because of the strong dissipation. The spectral analysis of the current time series gives the estimates of the NIO peak frequency as 0.0307 cph, i.e., $f_P = 0.98f$, implying a red-shift. The near-inertial wave has an upward phase velocity, which is estimated as 43 m day^{-1}, corresponding to a vertical wave length of about 58 m. The almost in-phase oscillation of the three stations indicates that the horizontal scale of the NIO is at least hundreds of kilometers. As the ADCP moorings were deployed after the typhoon's passage, the immediate oceanic response was not acquired, but the observed NIO event lasted for about 15 days.

The characteristics of the observed NIOs are influenced by the presence of the YCC and SCSWC. Since the northeastward background flow can interact with the upstream components of the NIOs, and the background vorticity is examined as negative, both the Doppler shift and shear flow modulation mechanisms can be responsible for the red-shift of the NIOs. With the present observation, however, we are unable to separate their effects. The NIOs triggered by hurricanes usually have a short sustaining period of several days, especially in the shallow areas with strong turbulence. However, the negative background vorticity broadens the frequency band for NIOs, which renders our study area a wave-guide. The trapping and amplification effects maintained the observed NIOs for as long as 15 days in July 2008.

The SCS has frequent typhoon events, which is a typical cause of oceanic NIOs. Based on this study, strong near-inertial currents could be dominant over other components in the SCS, implying a significant influence on the local sea surface height and turbulent mixing. Meanwhile the SCS has variable hydrographic structure and circulation because of the alternating monsoon winds. With different topography, oceanic stratification, background flow,

and atmospheric forcing, NIOs may have different characteristics. Therefore, to clarify the NIO behavior and finally predict NIO occurrences in the SCS, further efforts including field observations and numerical modeling are necessary.

References

Chaigneau A, Pizarro O, Rojas W (2008) Global climatology of near-inertial current characteristics from Lagrangian observations. Geophys Res Lett 35:L13603. doi:10.1029/2008GL034060

Chen S, Ma J (1991) Oceanographic data processing methods and its application. Ocean Publishing, Beijing, p 660 (in Chinese)

Chu PC, Veneziano JM, Fan CW, Carron MJ, Liu WT (2000) Response of the South China Sea to tropical cyclone Ernie. J Geophys Res 105:13991–14009

D'Asaro EA, Perkins H (1984) A near-inertial internal wave spectrum for the Sargasso Sea in late summer. J Phys Oceanogr 14:489–505

Deans SR (1983) The Radon transform and some of its applications. Wiley, Newyork, p 289

Fu LL (1981) Observations and models of inertial waves in the deep ocean. Rev Geophys Space Phys 19:141–170

Gill AE (1984) On the behavior of internal waves in the wake of storms. J Phys Oceanogr 14:1129–1151

Gonella J (1971) A local study of inertial oscillations in the upper layers of the ocean. Deep Sea Res 21:895–909

Hu J, Kawamura H, Hong H, Qi Y (2000) A review on the currents in the South China Sea: seasonal circulation, South China Sea Warm Current and Kuroshio intrusion. J Oceanogr 56:607–624

Hu J, Kawamura H, Li C, Hong H, Jiang Y (2010) Review on current and seawater volume transport through the Taiwan Strait. J Oceanogr 66:591–610

Kunze E (1985) Near-inertial wave propagation in geostrophic shear. J Phys Oceanogr 15:544–565

Leaman KD, Sanford TB (1975) Vertical energy propagation of inertial waves: a vector spectral analysis of velocity profiles. J Geophys Res 80:1975–1978

Mooers CNK (1975) Several effects of a baroclinic current on the cross-stream propagation of inertial-internal waves. Geophys Fluid Dyn 6:245–275

Orvik KA, Mork M (1995) A case study of Doppler-shifted inertial oscillations in the Norwegian Coastal Current. Cont Shelf Res 15:1369–1379

Park JJ, Kim K, King BA (2005) Global statistics of inertial motions. Geophy Res Lett 32:L14612. doi:10.1029/2005GL023258

Perkins H (1972) Inertial oscillations in the Mediterranean. Deep Sea Res 19:289–296

Perkins H (1976) Observed effect of an eddy on inertial oscillations. Deep Sea Res 23:1037–1042

Pollard RT (1970) On the generation by winds of inertial waves in the ocean. Deep Sea Res 17:795–812

Shay LK, Elsberry RL (1987) Near inertial ocean current response to hurricane Frederic. J Phys Oceanogr 17:1249–1269

Su J (2004) Overview of the South China Sea circulation and its influence on the coastal physical oceanography near the Pearl River Estuary. Cont Shelf Res 24:1745–1760

Webster F (1968) Observation of inertial period motions in the deep sea. Rev Geophys 6:473–490

Xie XH, Shang XD, Chen GY, Sun L (2009) Variations of diurnal and inertial spectral peaks near the bi-diurnal critical latitude. Geophys Res Lett 36:L02606. doi:10.1029/2008GL036383

Xu Z (1999) Dynamics of internal waves in the ocean. Science Press, Beijing, p 336

Zhang X, Liang X, Tian J (2005) Study on internal tides and near-inertial motions in the upper 450 m ocean in the northern South China Sea. Chin Sci Bull 50:2027–2031

Zheng Q, Lai RJ, Huang NE, Pan J, Liu TW (2006) Observation of ocean current response to 1998 Hurricane Georges in the Gulf of Mexico. Acta Oceanol Sin 25:1–14

Zhu D, Li L (2007) Near inertial oscillations in shelf break of northern South China Sea after passage of typhoon Wayne. J Trop Oceanogr 26:1–7 (in Chinese with English abstract)